Received: 20 September 2023 | Revised: 8 November 2023 | Accepted: 22 November 2023

DOI: 10.1002/jat.4570

RESEARCH ARTICLE

Journal of Applied Toxicology WILEY

Arzanol, a natural phloroglucinol α-pyrone, protects HaCaT keratinocytes against H_2O_2-induced oxidative stress, counteracting cytotoxicity, reactive oxygen species generation, apoptosis, and mitochondrial depolarization

Franca Piras[1] | Valeria Sogos[1] | Federica Pollastro[2,3] | Giovanni Appendino[2] | Antonella Rosa[1]

[1]Department of Biomedical Sciences, University of Cagliari, Monserrato, 09042, Italy

[2]Department of Pharmaceutical Sciences, University of Eastern Piedmont, Novara, 28100, Italy

[3]PlantaChem S.r.l.s, Novara, 28100, Italy

Correspondence
Franca Piras and Antonella Rosa, Department of Biomedical Sciences, University of Cagliari, Cittadella Universitaria, 09042 Monserrato, Cagliari, Italy.
Email: fpiras@unica.it and anrosa@unica.it

Funding information
Research Integrative Fund (FIR) of the University of Cagliari

Abstract

Skin oxidative stress results in structural damage, leading to premature senescence, and pathological conditions such as inflammation and cancer. The plant-derived prenylated pyrone–phloroglucinol heterodimer arzanol, isolated from *Helichrysum italicum* ssp. *microphyllum* (Willd.) Nyman aerial parts, exhibits anti-inflammatory, anticancer, antimicrobial, and antioxidant activities. This study explored the arzanol protection against hydrogen peroxide (H_2O_2) induced oxidative damage in HaCaT human keratinocytes in terms of its ability to counteract cytotoxicity, reactive oxygen species (ROS) generation, apoptosis, and mitochondrial membrane depolarization. Arzanol safety on HaCaT cells was preliminarily examined by the 3-(4,5-dimethylthiazol-2-yl)-2,5-diphenyltetrazolium bromide (MTT) assay and microscopic observation. The arzanol pre-incubation (5–100 μM, for 24 h) did not induce cytotoxicity and morphological alterations. The phloroglucinol, at 50 μM, significantly protected keratinocytes against cytotoxicity induced by 2 h-incubation with 2.5 and 5 mM H_2O_2, decreased cell ROS production induced by 1 h-exposure to all tested H_2O_2 concentrations (0.5–5 mM), as determined by the 2′,7′-dichlorodihydrofluorescein diacetate (H_2DCFDA) assay, and lipid peroxidation (thiobarbituric acid reactive substances [TBARS] method). The 2-h incubation of keratinocytes with H_2O_2 determined a significant increase of apoptotic cells versus control cells, evaluated by NucView® 488 assay, from the dose of 2.5 mM. Moreover, an evident mitochondrial membrane potential depolarization, monitored by fluorescent mitochondrial dye MitoView™ 633, was assessed at 5 mM H_2O_2. Arzanol pretreatment (50 μM) exerted a strong significant protective effect against apoptosis, preserving the mitochondrial membrane potential of HaCaT cells at the highest H_2O_2 concentrations. Our results validate arzanol as an antioxidant agent for the prevention/treatment of skin oxidative-related disorders, qualifying its potential use for cosmeceutical and pharmaceutical applications.

KEYWORDS
antioxidant activity, apoptosis, arzanol, H_2O_2 oxidative stress, HaCaT cells, ROS

1 | INTRODUCTION

Oxidative stress in biological systems was recently defined as a long-term and/or transient increase of steady-state reactive oxygen species (ROS) amounts that, leading to oxidative modifications of macromolecules, may terminate in cell death (Lushchak & Storey, 2021). ROS can be physiologically produced and, at appropriate levels, are indispensable for cell differentiation, apoptosis, and cell survival (Bae et al., 2011), and are involved in the maintenance of redox homeostasis. In addition to endogenous, ROS generation may be induced by exogenous stimuli (Liu, Cheng, et al., 2023).

The skin, the largest organ in humans, is involved in many physiological functions; however, its surface area is more vulnerable to environmental insults than other organs. Environmental pollution, increased ultraviolet (UV) radiation intensity, and xenobiotics can lead to skin oxidative stress (Liu, Tang, et al., 2023; Schikowski & Krutmann, 2019). ROS excess in the skin results in structural damage, inducing collagen degradation, lipid peroxidation, and increased cell membrane permeability. It can lead to skin premature senescence and inflammatory states, such as psoriasis and dermatitis. Moreover, the binding of ROS to DNA can activate proto-oncogenes and cancers, such as melanoma and squamous cell carcinoma (SCC, Bhat et al., 2015; Brand et al., 2018; Shimamoto et al., 2019). The skin opposes this through a proper antioxidant system, composed of enzymatic antioxidants, as well as non-enzymatic antioxidants (Baek & Lee, 2016). However, being the skin constantly subjected to exogenous oxidative insults, the use of external antioxidative substances may help to reduce oxidative damage, especially in skin pathological conditions that can be exacerbated by oxidative stress (Caliş et al., 2022; Shimamoto et al., 2019).

Among exogenous substances with antioxidant properties currently available, those derived from plants (polyphenols, tocopherols, carotenoids, ascorbic acid, as well as components of essential oils) may play a significant role in the defense and regenerative mechanisms of the free radical damaged skin (Calniquer et al., 2021; Michalak et al., 2023; Suroowan et al., 2023) acting on the skin by mechanisms of prevention, interception, and repair (Michalak, 2022). Many polyphenols, for example, can act as sunscreens and prevent the adverse effects of UV radiation on the skin (Nichols & Katiyar, 2010), whereas others can be radical scavengers, inhibitors of lipid peroxidation, lipoxygenases, and elastases, or promoters of the collagen and elastin fiber synthesis, showing anti-inflammatory, anti-allergic, anti-aging, and wound healing properties (Gülçin, 2010; Michalak, 2022; Saha et al., 2023).

Helichrysum italicum (Roth) G. Don is a Mediterranean plant, in popular medications used for various beneficial health effects and to treat different skin disorders (Furlan & Bren, 2023). The *H. italicum* ssp. *Microphyllum*, synonym of *Helichrysum microphyllum* Cambess. subsp *tyrrhenicum* Bacch., Brullo & Giusso (Ornano et al., 2015), an endemism of Sardinia, Corsica, and Balearic Island, was traditionally used as a dermoprotective product (Juliano et al., 2019). Its essential oil was found to have many properties, but the chemical profile and biological activity were different according to the area of collection (Angioni et al., 2003; Juliano et al., 2019; Ornano et al., 2015). Several secondary metabolites, such as phloroglucinols, acetophenones, pyrones, and sesquiterpenes, isolated from the aerial parts of this subspecies, exhibited anti-inflammatory (Appendino et al., 2007; Bauer et al., 2011) and antioxidant activity in several models of oxidative stress (Rosa et al., 2007, 2011, 2017). Among them, the naturally prenylated pyrone–phloroglucinol heterodimer arzanol (Figure 1) showed anti-inflammatory, anticancer, antimicrobial, and antioxidant activities (Appendino et al., 2007; Deitersen et al., 2021; Del Gaudio et al., 2018; Mammino, 2017; Rosa et al., 2007, 2017; Taglialatela-Scafati et al., 2013). The anti-inflammatory activity was explained by the inhibition of the activation of inflammatory transcription nuclear factor ƙB (NFκB) and the release of pro-inflammatory cytokines in lipopolysaccharide (LPS)-stimulated primary monocytes (Appendino et al., 2007). Arzanol inhibited the biosynthesis of pro-inflammatory lipid mediators like prostaglandin E_2 (PGE_2) also in an *in vivo* rat model suppressing the inflammatory response of the carrageenan-induced pleurisy (Bauer et al., 2011).

Arzanol was efficient in protecting different cell lines and animals from oxidative stress (Rosa et al., 2011, 2017) and also exhibited radical scavenging activity in various *in vitro* systems of lipid peroxidation, surpassing or competing with standard lipophilic antioxidants, like vitamin E, and hydrophilic ones, like vanillyl alcohol (Rosa et al., 2007, 2011).

The HaCaT cell line is a spontaneously immortalized human keratinocyte cell line from adult skin. These cells are physiologically similar to normal human keratinocytes and retain epidermal differentiation ability, reconstituting a stratified and differentiated epidermal structure after transplantation onto nude mice (Boukamp et al., 1988). HaCaT cells are extensively used as a model to study the oxidative stress in human epidermal cells, and the H_2O_2-induced HaCaT cell damage model has been extensively applied to find antioxidant effects of pharmacological treatment of skin pathologies (Bae et al., 2014; Liu, Tang, et al., 2023; Zhang et al., 2020).

Hydrogen peroxide is a small electroneutral molecule, generated in numerous biological processes, that reacts with transition metal

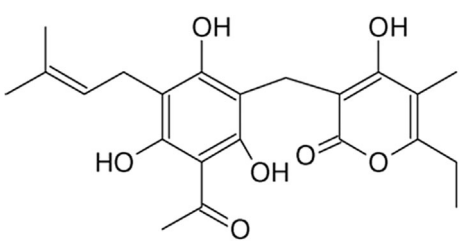

FIGURE 1 Chemical structure of arzanol.

centers, selenoproteins, and with thiol-based proteins, such as catalase, glutathione peroxidases, and peroxiredoxins (Winterbourn, 2013, 2018). H_2O_2 is widely used to induce oxidative damage in cellular models, and a strong production of ROS has been observed in H_2O_2-treated cells (Park et al., 2020; Zhang et al., 2020).

In light of these findings, the current study, for the first time, evaluated the protective effect of arzanol in HaCaT cells against H_2O_2-induced oxidative damage. To this goal, experiments were designed to evidence the ability of the phloroglucinol to reduce cytotoxicity and ROS generation because of the peroxide. In addition, the arzanol protection on apoptosis and mitochondrial membrane potential depolarization observed in oxidated HaCaT cells were also explored.

The results of this work were expected to provide indications on the nature of the molecular mechanism(s) underlying the antioxidative activity of arzanol, for future potential dermatological, cosmetic, and pharmaceutical applications in skin oxidative-related diseases and other related conditions.

2 | MATERIALS AND METHODS

2.1 | Materials

Cell culture materials, such as Dulbecco's Modified Eagle Medium (DMEM), fetal bovine serum (FBS), penicillin, streptomycin, and trypsin 0.25%-EDTA were all purchased from EuroClone (Pero, MI, Italy). Dimethyl sulfoxide (DMSO), 3-(4,5-dimethylthiazol-2-yl)-2,5-diphenyltetrazolium bromide (MTT), 2′,7′-dichlorodihydrofluorescein diacetate (H_2DCFDA), trichloroacetic acid (TCA), 2-thiobarbituric acid (TBA), and hydrogen peroxide (H_2O_2) solution 30% (w/w), were purchased from Merck Life Science (Milan, Italy). NucView® 488 and MitoView ™ 633 apoptosis assay kits were obtained from Biotium (Fremont, CA, USA).

2.2 | Arzanol extraction and isolation

Arzanol (Figure 1) was isolated from an acetone extract of *H. italicum* ssp. *Microphyllum*, collected in 2021 (Sardinia, Italy), according to literature (Appendino et al., 2007). A batch of the plant is stored in the phytochemistry laboratory of Novara (Italy) with the code HM-CA2021. Approximately 500 g of the dried aerial parts (leaves and flowerheads) were extracted two times with 2.5 L of acetone in a vertical percolator. After that, the extract was filtered under vacuum in a sintered filter to remove the vegetable material and the solvent was then evaporated with rotary evaporator to obtain a gummish residue. This latter residue was dissolved in EtOAc—petroleum ether solution 1:1 to promote the precipitation of arzanol. Characterization was made by spectroscopic methods (^{1}H NMR, ^{13}C NMR, UV, IR, and HR-MS), and the arzanol structure was confirmed by comparison of its physical properties with scientific data reported by Appendino et al. (2007). The final purity of arzanol was 98%.

2.3 | Cell culture

Human keratinocytes HaCaT cell line was obtained from CLS-Cell Line Services (Eppelheim, Germany). The cells were cultured in high glucose DMEM supplemented with 10% FBS, 100 units/mL of penicillin, and 100 μg/mL of streptomycin and kept at 37°C in a water-saturated humidified incubator at 5% CO_2. The cells were split once a week when the cells were confluent using Trypsin 0.25%-EDTA and were plated at a density of 1×10^5/mL and grown until reaching about 80% confluence in experimental studies.

2.4 | Cell viability (MTT) assay

The cytotoxicity of arzanol, DMSO, and H_2O_2 was performed by MTT assay as previously described (Kasugai et al., 1990; Petretto et al., 2023). HaCaT cells were seeded at a density of 10^4 cells/well in a 96-well plate in 100 μL of complete culture medium and incubated at 37°C in 5% CO_2 for 48 h. The cells were treated, at 80% confluence, for 24 h with arzanol (5–100 μM, from 10-mM stock solution in DMSO) in a complete fresh medium. After incubation, the medium was discarded and MTT reagent (0.5 mg/mL in DMEM) was added into each well, and then the plate was incubated for 3 h at 37°C. After reacting, the MTT solution was carefully removed from the culture plate, and the water-insoluble formazan crystals, formed in the cells, were solubilized by adding 100 μL of DMSO solvent into each well. The optical density of the formazan crystals was measured at 570 nm absorbance using spectrophotometry by an Infinite 200 Tecan microplate reader (Salzburg, Austria). Arzanol-treated cells were compared for viability to control cells (untreated). The optical density in untreated control cells was evaluated 100% alive, and viability data were reported in percentage of respective control cells. The effect on HaCaT viability of different amounts (from 0.05% to 1%) of DMSO (molecule vehicle), used to dissolve the phenolic compound, was also evaluated.

The cytotoxic effect of the oxidant H_2O_2 was evaluated in a different set of experiments. Cells, at about 80% confluence, were incubated for 2 h with different amounts of H_2O_2 (0.05, 0.1, 0.25, 0.5, 0.75, 1, 2.5, and 5 mM in complete medium) and then subjected to the MTT assay as above described.

The evaluation of the HaCaT cell morphology after incubation with arzanol, H_2O_2, or DMSO was performed by microscopic observation with a ZOE™ Fluorescent Cell Imager (Bio-Rad Laboratories, Inc., California, USA).

2.5 | Arzanol protection against H_2O_2 inducted cytotoxicity

MTT viability assay was also applied to determine the rate of protection of arzanol (24 h of pre-incubation) against the cytotoxic effect induced in HaCaT cells by H_2O_2 exposure. Cells were seeded at a density of 10^5 cells/mL in 96-well plates in a complete culture medium. After 48 h of incubation, the cells were treated with 50 μM

arzanol for 24 h. After the medium removal, keratinocytes were exposed for 2 h to different concentrations of H_2O_2 (from 0.5 to 5 mM, in DMEM solution) in the absence (oxidized controls) and in the presence of arzanol. Cells were then subjected to the MTT assay as described above. Viability data were expressed as a percentage of respective control cells (untreated cells). The effect of the maximal amount of DMSO (0.5%) was also evaluated in this system.

2.6 | Intracellular ROS assay

The redox status of HaCaT keratinocytes in response to H_2O_2 in the absence and in the presence of arzanol was determined. The intracellular ROS production was determined by the H_2DCFDA assay (Sogos et al., 2021), a method based on the structure of 2′-7′ dichlorofluorescein (DCF) that interacts with reactive species to lead to a fluorescence (Pavelescu, 2015). The acetyl groups of H_2DCFDA enable penetration through the cell membrane and, into the cell, cytoplasmic esterases cleave it, releasing the reduced state of DCF (DCF-H_2) which reacts with intracellular reactive species and fluoresces (Pavelescu, 2015; Petretto et al., 2023). HaCaT cells were seeded in 96-well plates at 10^5 cells/mL density in 100 μL/well of complete culture medium and cultured for 48 h. Then, fresh medium without (control cells) and with 50 μM arzanol was added, and cells were incubated for a further 24 h. Next, the cells, after washing with phosphate-buffered saline (PBS) solution (pH 7.4), were incubated with 10 μM H_2DCFDA in PBS, at 37°C for 30 min. After incubation, the H_2DCFDA solution was discharged, and cells were washed before the addition of PBS alone in control cells or different H_2O_2 concentrations (0.5, 1, 2.5, and 5 mM) in cells without (oxidized controls) and with arzanol pre-treatment. The effect on ROS generation was also evaluated in HaCaT cells after 24 h of incubation with only 50 μM arzanol. ROS production was detected and monitored (every 5 min) for 1 h by using an Infinite 200 Tecan microplate reader at a controlled temperature of 37°C. The reading was performed using an excitation wavelength of 490 nm and an emission wavelength of 520 nm. Data were collected and analysed using the Tecan I-control 1.5 V software. Fluorescence data were normalized to control cells.

2.7 | Thiobarbituric acid reactive substances (TBARS) assay

The antioxidant activity of arzanol against the H_2O_2 oxidation in HaCaT cells was also monitored by the evaluation of its effect on the level of low-molecular-weight end products (mainly malondialdehyde, MDA) (TBARS method), formed during the decomposition of primary lipid peroxidation products (Aguilar Diaz De Leon & Borges, 2020; Rosa et al., 2007). HaCaT cells were cultured in a complete culture medium in 60 mm plates and a density of 1.5×10^5 cells/mL in 4 mL/plate for 48 h. Afterwards, the cells were incubated in the absence (control cells) and in the presence of 50 μM arzanol in a fresh medium for another 24 h. After the medium removal and washing with PBS solution (pH 7.4), keratinocytes, without (oxidized controls) and with arzanol pre-treatment, were exposed for 1 h at 37°C to different concentrations of H_2O_2 (0.5, 1, 2.5, and 5 mM) in PBS solution. After PBS removal, 10% TCA (250 μL) was added and then cell pellets were transferred to a tube. Aliquots (500 μL) of 0.6% TBA were added, and cell samples were then incubated at 95°C for 45 min. After cooling on ice, the samples were centrifuged at 5000 rpm for 10 min, and the resulting pellets were dissolved in DMSO. TBARS production (Rosa et al., 2007) was detected using an Infinite 200 Tecan microplate reader. The reading was performed at 540 wavelengths. The collected data were analysed using the Tecan I-control 1.5 V software and normalized to control cells.

2.8 | Apoptosis and mitochondrial activity assay

The protective effect of arzanol against the changes in the mitochondrial membrane potential and apoptosis, inducted by H_2O_2 oxidation in HaCaT cells, was evaluated through the NucView® 488 and MitoView™ 633 Apoptosis Assay Kit, as previously reported (Sogos et al., 2021). NucView® 488 consists of a fluorogenic DNA dye and a DEVD substrate moiety. This complex, both non-fluorescent and non-functional, crosses the cellular membrane, and it can be cleaved by caspase-3/7 in the cytoplasm to release a high-affinity DNA dye that, after migration to the nucleus, dyes DNA with green fluorescence. MitoView™ 633, a far-red fluorescent mitochondrial dye, enters the cell and accumulates in mitochondria, becoming fluorescent with staining dependently on the potential of the mitochondrial membrane (higher in healthy cells and lower in apoptotic cells) (Sogos et al., 2021). HaCaT cells were seeded onto 96-well plates at 10^5 cells/mL and incubated for 48 h. Then, cells were treated for 24 h with 50 μM arzanol in a fresh medium. After incubation, the medium was carefully removed and cells were treated with NucView® 488 and MitoView™ 633 (mitochondrial dye) probes, according to the manufacturer's instructions, and different concentrations of H_2O_2 (0.25, 0.5, 0.75, 1, 2.5, and 5 mM) in fresh medium and then incubated at 37°C. The microscopic observations were finally made after 2 and 24 h of incubation using a ZOE™ Fluorescent Cell Imager. Instrument gain and offset values were adjusted using control (untreated cells) and remained constant for all subsequent experiments. Image analysis of NucView® 488 and MitoView™ 633 images was performed with ImageJ software (version 1.53e). Briefly, background fluorescence was subtracted from images, and histogram values of fluorescence intensity were expressed as percent of control cell fluorescence. For each sample, eight images (from two different experiments) were processed for image analysis.

2.9 | Statistical analysis

All data were preliminary assessed for normal distribution with Graph Pad INSTAT software (GraphPad Software, San Diego, CA, USA). Data are presented as mean ± standard deviation (SD) of three independent experiments with different replicates. Multiple and two groups of data

comparison were analysed using one-way analysis of variance (ANOVA) with Bonferroni post test and Student's unpaired *t*-test with Welch's correction, respectively. The tests were carried out using Graph Pad INSTAT software. Differences were considered statistically significant when the *p*-value was less than 0.05.

3 | RESULTS

3.1 | Effect on HaCaT cell viability (MTT assay)

The cytotoxic potential of arzanol was evaluated by using the colorimetric MTT assay, a method frequently used as an indicator of cell viability, proliferation, and cytotoxicity (Petretto et al., 2023). Figure 2 shows the viability, expressed as percent of the control, induced by incubation for 24 h with different amounts of arzanol (5–100 μM) (Figure 2A) and DMSO (0.05–1%) (Figure 2B) in HaCaT cells.

The results of this test (Figure 2A) showed that arzanol, after 24 h of incubation, did not decrease HaCaT cell viability at concentrations from 5 to 100 μM with regard to control cells. DMSO, used to dissolve arzanol, did not affect cell viability from 0.05% to 0.5%, whereas a 21% significant reduction in viability ($p < 0.01$ versus control cells) was observed at 1% (Figure 2B).

Based on these data, a 50-μM concentration of arzanol, containing 0.5% of DMSO, was used as the tested maximal concentration of the phloroglucinol in successive experiments.

Figure 2C shows representative images of phase contrast microscopy of control HaCaT cells and cells treated for 24 h with arzanol 50 μM or DMSO 0.5%. Control (untreated) keratinocytes, at a non-complete confluency, appeared enlarged, elongated, and linked to each other. The arzanol treatment did not induce, from 5 to 50 μM, a change in cell morphology and a reduction in the cell number, and treated cells appeared very similar to control cells. The vehicle molecule DMSO did not affect HaCaT cell morphology from 0.05% to 0.5%, and DMSO-treated cells showed the same microscopic features as control cells.

MTT assay was also applied to evaluate the H_2O_2 effect on HaCaT cell viability. Figure 3A shows the viability (as percent of the control) induced by 2 h-incubation with different amounts of H_2O_2 (0.05–5 mM) in HaCaT cells, whereas the corresponding morphological images of phase contrast microscopy are reported in Figure 3B.

The exposure to H_2O_2 did not markedly change the viability rate with respect to control cells from 0.05 to 0.25 mM of oxidant. At higher tested concentrations (from 0.5 to 5 mM), H_2O_2 induced a significant cytotoxic effect in a concentration-dependent manner, with cell viability reduction values in the range of 21–83%.

Microscopic observations (Figure 3B) did not show an evident cell morphology and density alteration in the H_2O_2 dose range of 0.05–0.75 mM, whereas, at the high concentrations, areas with a decreased cell density and cell-to-cell packing were noted. Moreover, some cells displayed an ill-defined cytoplasm, changes in size, pyknotic nuclei, and fragmentation.

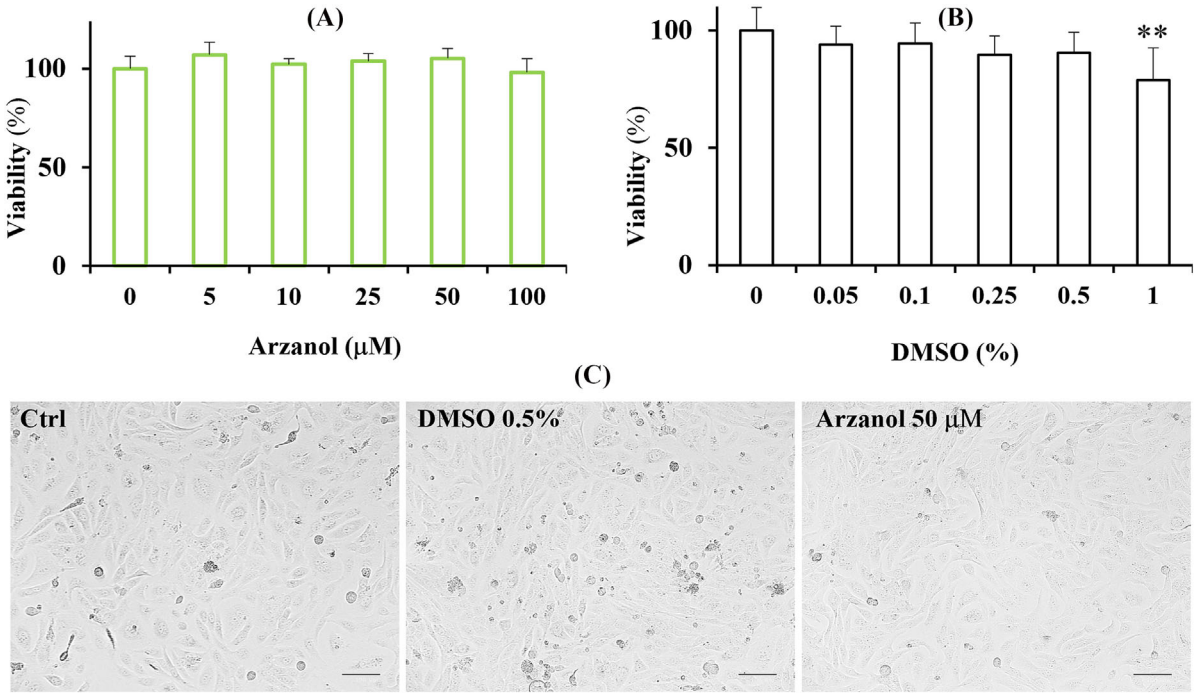

FIGURE 2 Viability, expressed as percent of the control (0), induced by incubation for 24 h with different amounts of arzanol (5–100 μM) (A) and DMSO (0.05–1%) (B) in HaCaT cells (MTT assay). Three independent experiments are performed, and data are presented as mean and SD ($n = 15$). ** = $p < 0.01$ versus 0. Statistical significance of differences was assessed by one-way ANOVA and Bonferroni post test. (C) The panel shows representative images of phase contrast of control HaCaT cells (Ctrl) and cells treated for 24 h with arzanol 50 μM or DMSO 0.5%. Bar = 100 μm. DMSO, dimethyl sulfoxide; MTT, 3-(4,5-dimethylthiazol-2-yl)-2,5-diphenyltetrazolium bromide.

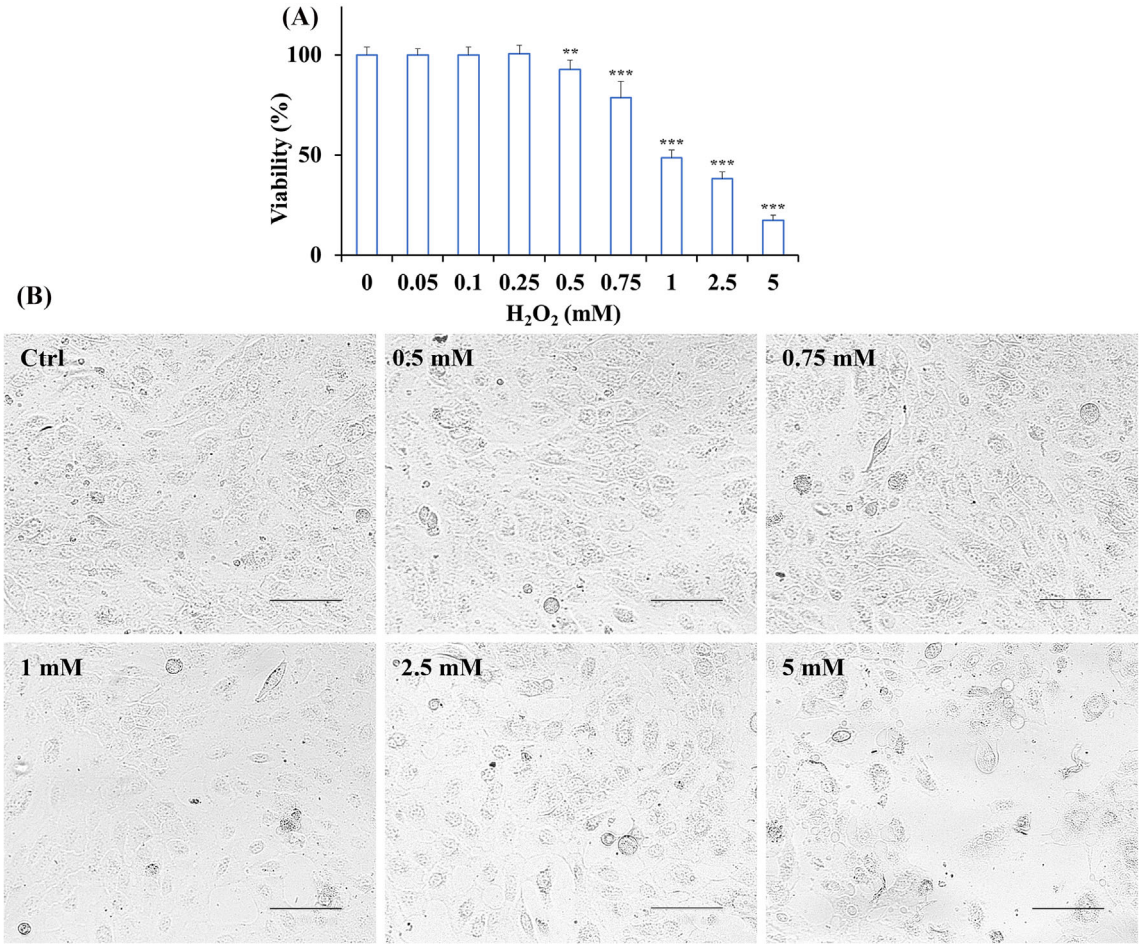

FIGURE 3 (A) Viability, expressed as percent of the control (Ctrl), induced by incubation for 2 h with different amounts of H_2O_2 (0.05–5 mM) in HaCaT cells (MTT assay). Three independent experiments are performed, and data are presented as mean and SD ($n = 15$). *** = $p < 0.001$, ** = $p < 0.01$ versus Ctrl. Statistical significance of differences was assessed by one-way ANOVA and Bonferroni post test. (B) The panel shows representative images of phase contrast of control HaCaT cells (Ctrl) and cells treated for 2 h with the different amounts of H_2O_2 (0.05–5 mM). Bar = 100 µm. ANOVA, analysis of variance; MTT, 3-(4,5-dimethylthiazol-2-yl)-2,5-diphenyltetrazolium bromide.

3.2 | Arzanol protection against H_2O_2 inducted cytotoxicity

The arzanol protection against H_2O_2-inducted cytotoxicity was then assessed by MTT assay.

Figure 4 shows the viability, expressed as percent of control cells, induced by 2-h incubation with different amounts of H_2O_2 (0.5–5 mM) in HaCaT cells measured in control oxidized samples (OX) and in samples oxidized after a 24 h-pre-incubation with 50 µM arzanol.

A slight viability reduction was observed in the range of 0.5–1 mM H_2O_2 concentration both in the absence and in the presence of arzanol. A significant protection against H_2O_2-induced cytotoxicity was evident at the H_2O_2 concentrations of 2.5 mM ($p < 0.01$ versus the respective oxidized control) and 5 mM ($p < 0.05$), with arzanol-treated cells showing viability, with respect to control cells, of about 55–58%.

3.3 | Intracellular ROS

The effect of arzanol against the intracellular ROS generation induced in HaCaT keratinocytes by the H_2O_2 treatment was determined by the H_2DCFDA assay.

Figure 5 shows the ROS-induced fluorescence, expressed as percent of the control, measured during 1 h in HaCaT control cells, cells pre-incubated with arzanol 50 µM, and cells exposed to different amounts of H_2O_2 (0.5, 1, 2.5, and 5 mM) in the absence (oxidized samples) and in the presence of arzanol 50 µM (after 24 h-pre-incubation).

The H_2O_2-treatment induced a significant ($p < 0.001$) increase in cell fluorescence during 60 min time of exposure compared to the ROS basal level of control cells, and the highest relative intensity of fluorescence was observed in HaCaT keratinocytes at 5-mM concentration.

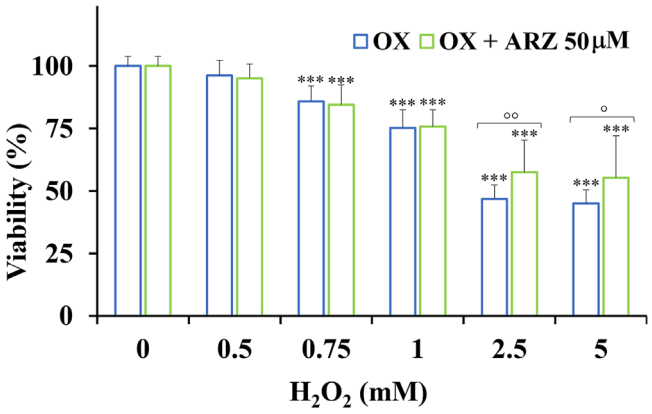

FIGURE 4 Viability, expressed as percent of control cells (0), induced by incubation for 2 h with different amounts of H_2O_2 (0.5–5 mM) in HaCaT cells measured in control oxidized samples (OX) and in samples oxidized after a 24 h-pre-incubation with 50 µM arzanol (MTT assay). Three independent experiments are performed, and data are presented as mean and SD ($n = 21$). *** = $p < 0.001$ versus control (0) (one-way ANOVA and Bonferroni post test); °° = $p < 0.01$, ° = $p < 0.05$ between oxidized cells in the absence and in the presence of 50 µM arzanol (Student's unpaired *t*-test with Welch's correction). ANOVA, analysis of variance; MTT, 3-(4,5-dimethylthiazol-2-yl)-2,5-diphenyltetrazolium bromide.

The pre-treatment for 24 h with arzanol 50 µM significantly ($p < 0.001$) reduced ROS production with respect to H_2O_2-oxidized HaCaT cells at all oxidation times and oxidant concentrations, and keratinocytes treated with the natural phenolic compound showed a fluorescence emission intensity similar to that of control HaCaT cells.

Interestingly, the treatment with only 50 µM arzanol for 24 h did not induce ROS generation in HaCaT cells and, at the lowest times of incubation (0–40 min), measured fluorescence was lower than the redox basal status, indicating a role of the compound in the ROS production mechanisms.

3.4 | TBARS assay

The arzanol antioxidant activity against the formation of secondary products of lipid peroxidation induced by H_2O_2 in HaCaT cells was monitored by TBARS method. Figure 6 shows TBARS formation, expressed as percent of the control, measured in control cells, cells pre-incubated with arzanol 50 µM, and cells exposed for 1 h to different amounts of H_2O_2 (0.5, 1, 2.5, and 5 mM) in the absence and in the presence (after 24 h-pre-incubation) of arzanol 50 µM. The exposure to H_2O_2 induced a concentration-dependent rise in the secondary lipid oxidative products, and a marked significant ($p < 0.001$) increase (188% with respect to control cells) was observed at the highest H_2O_2 tested concentrations (5 mM).

The cells treated with arzanol showed TBARS values similar to control cells at all the H_2O_2 tested concentrations, exhibiting significant protection versus the corresponding H_2O_2-oxidized cells at 2.5 ($p < 0.05$) and 5 mM ($p < 0.001$).

3.5 | Apoptosis and mitochondrial activity

Finally, the effect of arzanol against apoptosis and changes in the mitochondrial membrane potential induced by H_2O_2 oxidation in HaCaT cells was evaluated.

Figure 7A shows images of phase contrast, red emission (MitoView 633), and green emission (NucView 488) obtained for HaCaT control cells, cells pre-incubated with arzanol 50 µM, and H_2O_2-oxidized cells in the absence and in the presence of arzanol 50 µM (24 h-pre-incubation).

Quantitative data of fluorescence intensity (expressed as a percentage of control cells) are depicted in Figure 7B.

Observations made after 2 h of incubation with the oxidant ascertained a slight increase, with respect to control cells, of the apoptotic signal (green staining) in cells incubated with H_2O_2 from 0.5 to 1 mM, whereas the treatment with 2.5 and 5 mM H_2O_2 determined a significant ($p < 0.001$) increase in apoptotic cell number compared to the control, with values of 260% and 1031% of control, respectively. Moreover, associated altered cell morphology (brightfield) was observed at the highest tested H_2O_2 concentrations. H_2O_2 oxidation did not induce an evident change in the red fluorescence signal in the range of 0.5–2.5 mM, whereas the dose of 5 mM markedly reduced the red emission, indicating a depolarization of mitochondrial membrane potential.

Interestingly, a strong significant ($p < 0.001$) protective effect of arzanol 50 µM was evident against apoptosis induced in HaCaT cells by 5 mM H_2O_2, and arzanol-treated cells showed a fluorescent intensity of 280%, about three times lower than the corresponding oxidized sample. However, the arzanol treatment reduced, unless not significantly, the green signal also at the other oxidant doses.

Moreover, the phloroglucinol preserved HaCaT cells against mitochondrial membrane depolarization induced by 5 mM H_2O_2 addition, with arzanol-treated cells showing red fluorescence intensity similar to that of control cells.

HaCaT cells treated with only 50 µM arzanol for 24 h showed a lower apoptotic profile than control cells.

These results demonstrated a protective role of arzanol in HaCaT cells against apoptosis and mitochondrial membrane depolarization induced by H_2O_2 oxidation.

4 | DISCUSSION

Arzanol, a prenylated phloroglucinylpyrone isolated from leaves and flowerheads of *H. italicum* ssp. *microphyllum*, exhibited anti-inflammatory, antiviral, and antioxidant properties in different *in vitro* and *in vivo* models (Appendino et al., 2007; Rosa et al., 2007, 2017). For the first time, in this study, the antioxidant effect of arzanol was evaluated in human HaCaT keratinocytes against the oxidative stress induced by H_2O_2 with the aim of exploring its beneficial potential effects on human skin oxidative conditions. Cultured human HaCaT cells, being physiologically similar to normal human keratinocytes, represent a cell model amply used to assess the protective effect of

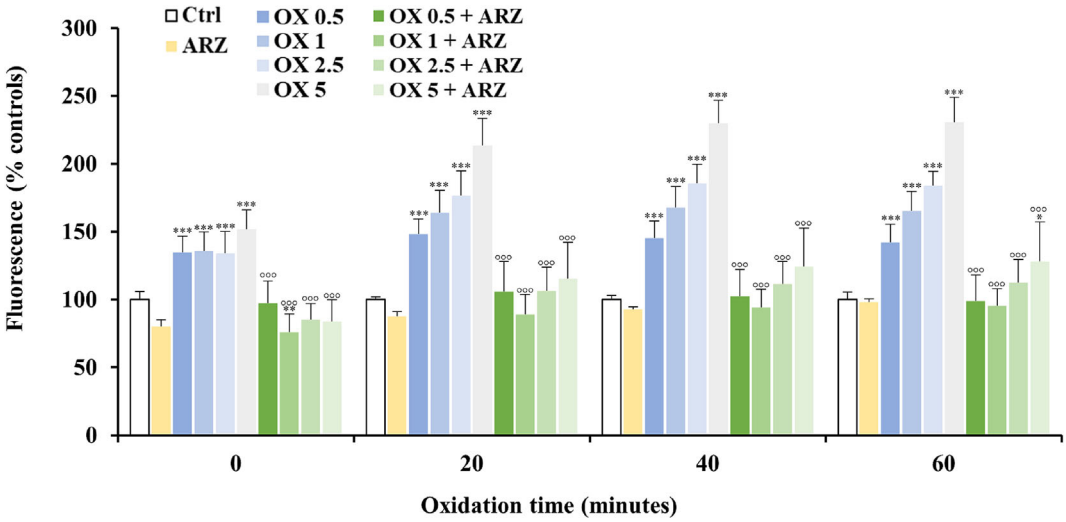

FIGURE 5 ROS-induced fluorescence, expressed as percent of the control (Ctrl), measured for 1 h, at different time points, in HaCaT control cells (Ctrl), cells pre-incubated with arzanol 50 μM (ARZ), and cells exposed to different amounts of H_2O_2 (0.5, 1, 2.5, and 5 mM) in the absence (oxidized samples, OX) and in the presence (after 24 h-pre-incubation) of arzanol 50 μM (OX + ARZ). Three independent experiments are performed, and data are presented as mean and SD ($n = 9$). Evaluation of the statistical significance of differences between groups was performed by one-way ANOVA followed by the Bonferroni multiple comparisons test. At each time point: *** = $p < 0.001$, ** = $p < 0.01$, * = $p < 0.05$ versus the respective Ctrl; °°° = $p < 0.001$ versus the respective OX samples. ANOVA, analysis of variance; ROS, reactive oxygen species.

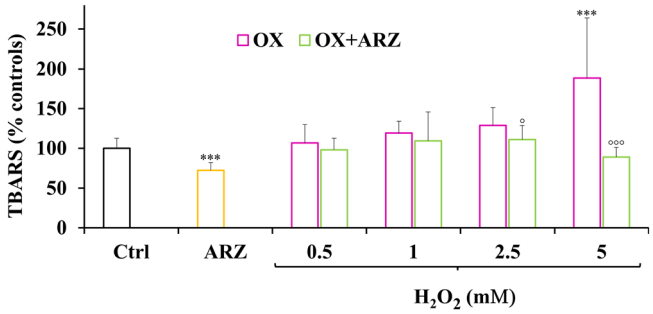

FIGURE 6 TBARS formation, expressed as percent of the control (Ctrl), measured in HaCaT control cells (Ctrl), cells pre-incubated with arzanol 50 μM (ARZ), and cells exposed for 1 h to different amounts of H_2O_2 (0.5, 1, 2.5, and 5 mM) in the absence (oxidized samples, OX) and in the presence (after 24 h-pre-incubation) of arzanol 50 μM (OX + ARZ). Three independent experiments are performed, and data are presented as mean and SD (n = 12). *** = $p < 0.001$ versus the Ctrl (one-way ANOVA and Bonferroni post test); °°° = $p < 0.001$, ° = $p < 0.05$ between oxidized cells in the absence and in the presence of 50 μM arzanol (Student's unpaired *t*-test with Welch's correction). TBARS, thiobarbituric acid reactive substances.

natural extracts and compounds against oxidative stress in human epidermal cells and skin pathologies (Jiang et al., 2020; Mirata et al., 2023; Wang et al., 2022). In our experimental conditions, HaCaT cells were cultured in DMEM medium containing high calcium (Ca^{2+}) amount, a condition favorable for keratinocyte differentiation (Colombo et al., 2017). Calcium represents one of the most important inductors of keratinocyte differentiation in the epidermis, increasing from the basal to the granular layer (Colombo et al., 2017).

At first, the cytotoxicity of arzanol on HaCaT cells was examined after 24 h of incubation. The results of the MTT assay showed that, at all tested concentrations, arzanol was not toxic for HaCaT cells. Moreover, confirming this, no difference in morphology was observed between arzanol-treated and control cells. According to our results, previous studies showed no cytotoxic effects of arzanol in peripheral blood mononuclear cells, obtained from healthy adult donors (Bauer et al., 2011), immortalized Vero cell line, and differentiated CaCo-2 cells (Rosa et al., 2011), as a model of the intestinal epithelium. Conversely, the phloroglucinol showed the ability to decrease viability in cancer cells as epithelial cancer cell lines (A549, RT-112, HeLa, CaCo-2) and B16F10 melanoma cells (Bauer et al., 2011; Deitersen et al., 2021; Rosa et al., 2017), indicating its selective cytotoxicity versus tumoral cells, maybe interacting with targets of the cell proliferation and survival signaling pathways (Rosa et al., 2017).

Then, the protective effect of 50 μM arzanol (after 24 h of pre-incubation) was assessed by MTT assay against the rate of cytotoxicity induced in HaCaT cells by 2 h oxidation with the peroxide H_2O_2. In our experimental conditions, the exposure of keratinocytes to H_2O_2 markedly reduced viability in a concentration-dependent manner from the dose of 0.75 to 5 mM, with a range of 30–50% cell viability observed at 1 mM. A dose-dependent decrease in HaCaT cell viability was previously reported in HaCaT cells exposed to H_2O_2 (100–500 μM) for 12 h, by MTT assay, with a 50% cell mortality at the concentration of 350 μM H_2O_2 (Zhang et al., 2020), whereas a survival rate of about 60% was reported by Park et al. (2020) for HaCaT cells exposed to 500 μM H_2O_2 for 24 h. In our study, the H_2O_2 cytotoxic effect was also confirmed by microscopic observation, which allowed to assess the presence of apoptotic features and decreased cell density. Similar

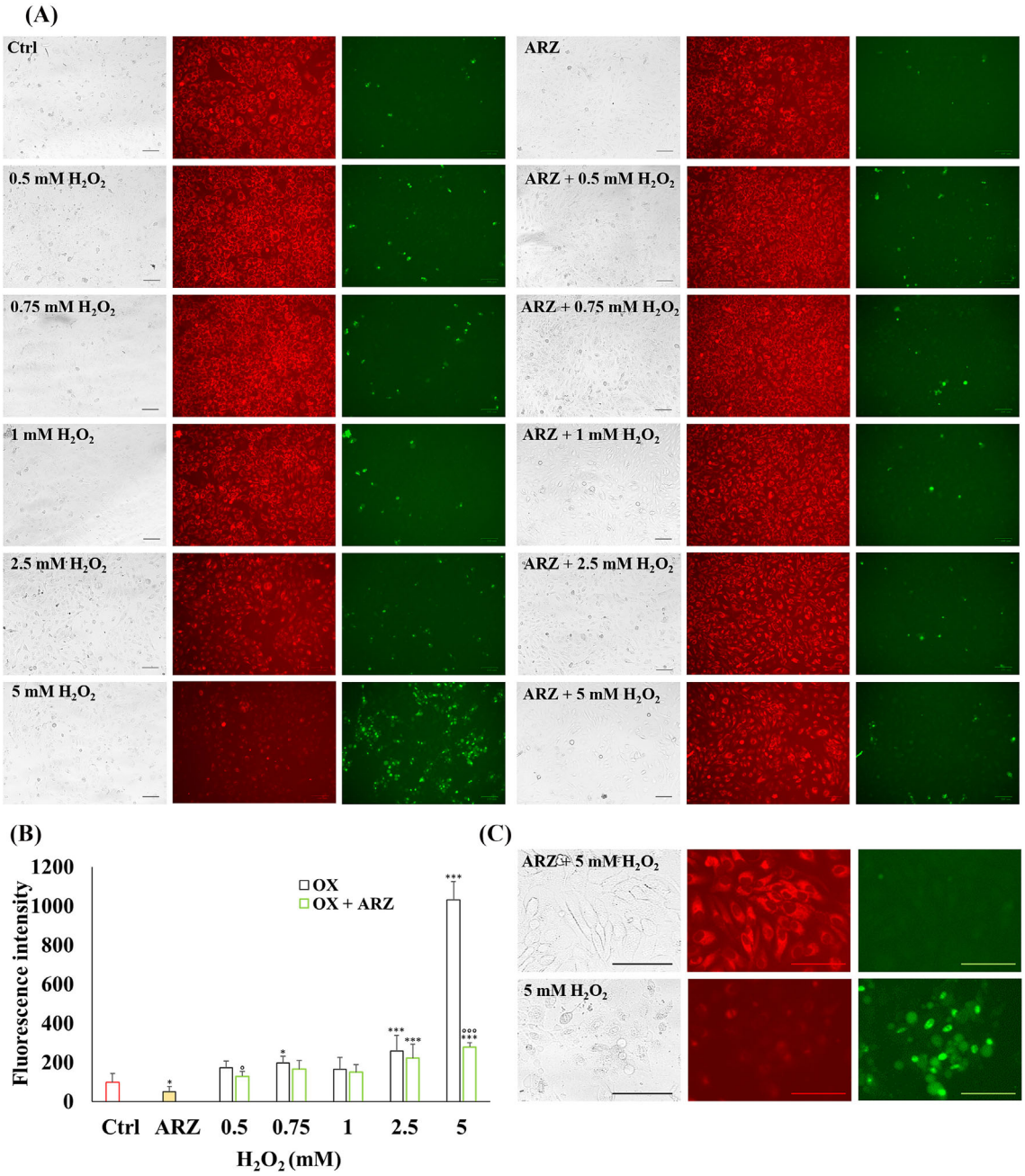

FIGURE 7 (A) Representative images of phase contrast, red emission (MitoView 633, polarized mitochondria dye), and green emission (NucView 488, caspase-3 substrate) and (B) fluorescent intensity (expressed as percent of Ctrl) obtained for HaCaT control cells (Ctrl), cells pre-incubated with arzanol 50 μM (ARZ), and cells exposed to different amounts of H_2O_2 (0.5, 0.75, 1, 2.5, and 5 mM) in the absence (oxidized samples, OX) and in the presence (after 24-h-pre-incubation) of arzanol 50 μM (OX + ARZ). Two independent experiments are performed, and data are presented as mean and SD ($n = 8$). *** = $p < 0.001$, * = $p < 0.05$ versus the Ctrl (one-way ANOVA and Bonferroni post test); °°° = $p < 0.001$, ° = $p < 0.05$ between oxidized cells in the absence and in the presence of 50 μM arzanol (Student's unpaired *t*-test with Welch's correction). (C) Magnification of a representative area from images relative to 5 mM H_2O_2 with and without arzanol. Bar = 100 μm. ANOVA, analysis of variance.

morphological alterations were observed in other cell types exposed to H_2O_2-damage, such as human umbilical vein endothelial cells, neuroblastoma cell line SK-N-MC, and HepG2 cells (Bayati et al., 2011; Farshori et al., 2021; Liao et al., 2022). Pre-treatment with arzanol preserved HaCaT cells from H_2O_2 cytotoxicity, and significant greater cell viability was observed in arzanol-treated cells in comparison with those no-treated exposed to the highest concentrations of oxidants. It was found that H_2O_2 lowered HaCaT cell viability by triggering DNA damage and mitochondria-mediated apoptosis by promoting ROS production (Park et al., 2020).

H_2O_2 is widely used to induce oxidative damage in cellular models (Park et al., 2020; Zhang et al., 2020). Because of its small size

and lack of charge, H_2O_2 crosses through the membrane barrier, so exposed cells cannot block its entry, and, in vivo, can diffuse over long distances into different organs (Lenzen et al., 2022; Mahaseth & Kuzminov, 2017). In the cells, H_2O_2 can interact with free Fe^{2+} ions and hydroxyl radical ($HO^{\bullet}$) are produced by Fenton's reaction, which is thought to be the main mechanism for oxidative damage (Bae et al., 2014; Bayati et al., 2011; Ransy et al., 2020; Yan et al., 2022). The $HO^{\bullet}$ radicals are extremely toxic, highly reactive with an ultrashort half-life (10^{-9} s), and capable of destroying any biological structure; however, their action is limited to the site of generation (Lenzen et al., 2022; Mahaseth & Kuzminov, 2017). Hydroxyl radicals damage DNA, acting on aromatic structures of RNA/DNA purines and pyrimidines by addition reactions at double bonds, attack sugars such as deoxyribose of DNA, and can act on biological membranes by the oxidative attack on polyunsaturated lipids by hydrogen extraction, triggering the autocatalytic process of lipid peroxidation (Bayati et al., 2011; Lenzen et al., 2022; Mahaseth & Kuzminov, 2017).

In this study, the H_2O_2 oxidation significantly induced a dose-dependent ROS increase (H_2DCFDA assay) in keratinocytes during 1 h of exposure, compared to the basal level of control cells, in line with previous studies (Park et al., 2020; Zhang et al., 2020). Pre-incubation for 24 h with arzanol 50 μM significantly reduced ROS production with respect to H_2O_2-oxidized HaCaT cells at all oxidation times and tested oxidant concentrations, confirming the antioxidant properties of this phloroglucinol. Interestingly, the treatment with arzanol 50 μM significantly reduced the level of internal physiologically ROS generation in HaCaT cells with respect to control cells.

Then, the protective effect of arzanol against the lipid peroxidation induced by H_2O_2 in HaCaT cells was monitored by TBARS assay. TBARS analysis is amply used to measure the formation of the secondary byproduct of lipid peroxidation, primarily composed of MDA (Aguilar Diaz De Leon & Borges, 2020). Our data showed a significant antioxidant activity of arzanol against lipid peroxidation, with a remarkable reduction in TBARS generation, evident at the highest H_2O_2 concentrations.

According to our findings, previous studies evidenced the antioxidant properties of the natural compound arzanol in different *in vitro* chemical systems of lipid peroxidation and in cultured cell models of oxidative stress. The phenolic compound preserved the oxidative modification of pure lipids (linoleic acid and cholesterol), liposomes, and human low-density lipoprotein (LDL), reducing the formation of their oxidative products (hydroperoxides, oxysterols, and MDA), due to its noteworthy efficacy in scavenging lipid peroxyl radicals ($ROO^{\bullet}$) because of hydrogen atom donor properties (Rosa et al., 2007, 2011). Moreover, arzanol, at non-cytotoxic concentrations, exerted noteworthy protection on tert-butyl hydroperoxide (TBH)-induced oxidative damage in a line of fibroblasts derived from monkey kidney (Vero cells) and in human intestinal epithelial cells (Caco-2) (Rosa et al., 2007, 2011). The antioxidant activity of arzanol was demonstrated also in the ferric–nitrilotriacetate (Fe-NTA) model of *in vivo* oxidative stress. Fe–NTA administration induces in animals a state of sustained oxidative stress in association with iron excess that leads to high production of free radicals, especially $HO^{\bullet}$ radicals (Rosa et al., 2005, 2017). The intraperitoneal administration of arzanol exerted a protective effect on the oxidative degradation of plasmatic

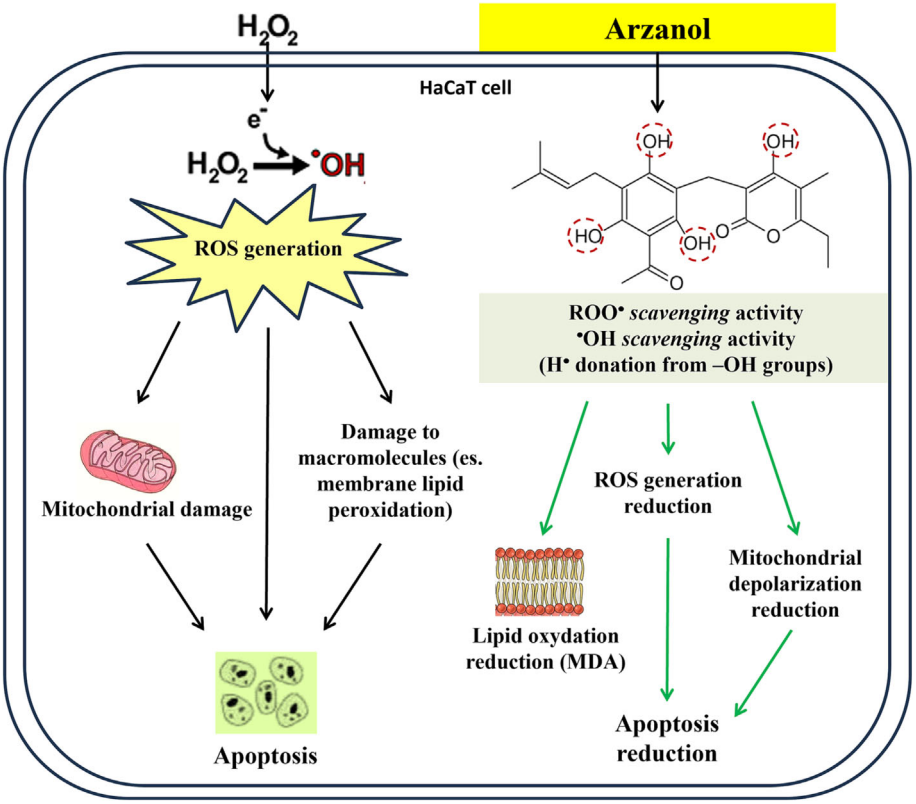

SCHEME 1 Schematic representation of the protective effect of arzanol against H_2O_2-induced oxidative stress in in HaCaT cells.

lipids induced by Fe-NTA at 1 h of oxidation (Rosa et al., 2017). The observed protective effect of arzanol in HaCaT cells was probably attributable to its scavenging ability against the H_2O_2-induced production of $HO^•$ and $ROO^•$ radicals.

Previous studies evidenced that the ROS production by the H_2O_2 oxidation induces mitochondria-mediated apoptosis (Park et al., 2020; Zhang et al., 2020). An increase in apoptotic cells (approximately nine-fold higher than control cells) was previously reported for HaCaT cells exposed to 500 μM H_2O_2 for 24 h (Park et al., 2020). Moreover, an increase (2.4-fold) in the caspase-3 expression was reported in HaCaT cells after 4 h of exposure to 350 μM H_2O_2 (Zhang et al., 2020), coupled with a marked decrease in the mitochondrial membrane potential. Mitochondrial membrane potential drop is a landmark event of early apoptosis, and the expression of caspase-3 protein promoted the acceleration of the mitochondrial apoptotic pathway (Sogos et al., 2021; Zhang et al., 2020). Therefore, the protective effect of arzanol against the apoptosis induced by H_2O_2 in HaCaT cells was evaluated, in this study, by NucView® 488 assay, which detects caspase-3/7 activity, whereas changes in the mitochondrial membrane potential were monitored by MitoView™ 633, a far-red fluorescent mitochondrial dye. The 2-h incubation of HaCaT cells with H_2O_2 determined a significant increase, with respect to control cells, of apoptotic cells from the dose of 2.5 mM, and an evident depolarization of mitochondrial membrane potential at 5 mM. Arzanol, at 50 μM, exerted a strong significant protective effect against apoptosis, preserving the mitochondrial membrane potential of HaCaT cells at the highest H_2O_2 concentration.

Our results highlighted the ability of the natural phenol arzanol to protect HaCaT cells against H_2O_2-induced oxidative stress. A summary of arzanol activity reported in this study is shown in Scheme 1.

5 | CONCLUSION

For the first time, in this study, the phloroglucinol α-pyrone arzanol showed a significant protective effect against H_2O_2-induced oxidative damage in HaCaT keratinocytes, a cell model extensively used to study the oxidative stress in human epidermal cells. The natural phenolic compound, at not-cytotoxic concentrations, showed the ability to preserve keratinocytes from the H_2O_2-induced viability reduction. Moreover, arzanol exhibited the capacity to reduce ROS generation probably acting as a scavenger of toxic $HO^•$ radicals, the main species of H_2O_2 damage, and $ROO^•$ from the oxidative attack to biological membranes, maybe acting as a hydrogen atom donor. In addition, the compound counteracted apoptosis and mitochondrial membrane potential depolarization. Taken together, these results furnished information about the potential use of arzanol for future cosmeceutical and pharmaceutical applications in skin oxidative-related diseases and other related conditions. However, further investigations are essential to clarify the mechanism of arzanol absorption and metabolism in HaCaT cells and to confirm these results *in vivo*.

ACKNOWLEDGMENTS

The study was supported by the Research Integrative Fund (FIR) of the University of Cagliari to V.S.—year 2020.

CONFLICT OF INTEREST STATEMENT

All authors declare they have no actual or potential competing interests.

DATA AVAILABILITY STATEMENT

The data that support the findings of this study are available from the corresponding author upon reasonable request.

ORCID

Franca Piras https://orcid.org/0000-0002-9010-1926
Valeria Sogos https://orcid.org/0000-0002-4021-1043
Federica Pollastro https://orcid.org/0000-0002-0949-2799
Giovanni Appendino https://orcid.org/0000-0002-4170-9919
Antonella Rosa https://orcid.org/0000-0003-0939-9364

REFERENCES

Aguilar Diaz De Leon, J., & Borges, C. R. (2020). Evaluation of oxidative stress in biological samples using the thiobarbituric acid reactive substances assay. *Journal of Visualized Experiments*, *12*(159). https://doi.org/10.3791/61122

Angioni, A., Barra, A., Arlorio, M., Coisson, J. D., Russo, M. T., Pirisi, F. M., Satta, M., & Cabras, P. (2003). Chemical composition, plant genetic differences, and antifungal activity of the essential oil of *Helichrysum italicum* G. Don ssp. *microphyllum* (Willd) Nym. *Journal of Agricultural and Food Chemistry*, *51*(4), 1030–1034. https://doi.org/10.1021/jf025940c

Appendino, G., Ottino, M., Marquez, N., Bianchi, F., Giana, A., Ballero, M., Sterner, O., Fiebich, B. L., & Munoz, E. (2007). Arzanol, an anti-inflammatory and anti-HIV-1 phloroglucinol alpha-pyrone from *Helichrysum italicum* ssp. *microphyllum*. *Journal of Natural Products*, *70*(4), 608–612. https://doi.org/10.1021/np060581r

Bae, S., Lee, E. J., Lee, J. H., Park, I. C., Lee, S. J., Hahn, H. J., Ahn, K. J., An, S., & An, I. S. (2014). Oridonin protects HaCaT keratinocytes against hydrogen peroxide-induced oxidative stress by altering microRNA expression. *International Journal of Molecular Medicine*, *33*(1), 185–193. https://doi.org/10.3892/ijmm.2013.1561

Bae, Y. S., Oh, H., Rhee, S. G., & Yoo, Y. D. (2011). Regulation of reactive oxygen species generation in cell signaling. *Molecules and Cells*, *32*(6), 491–509. https://doi.org/10.1007/s10059-011-0276-3

Baek, J., & Lee, M. G. (2016). Oxidative stress and antioxidant strategies in dermatology. *Redox Report: Communications in Free Radical Research*, *21*(4), 164–169. https://doi.org/10.1179/1351000215Y.0000000015

Bauer, J., Koeberle, A., Dehm, F., Pollastro, F., Appendino, G., Northoff, H., Rossi, A., Sautebin, L., & Werz, O. (2011). Arzanol, a prenylated heterodimeric phloroglucinyl pyrone, inhibits eicosanoid biosynthesis and exhibits anti-inflammatory efficacy in vivo. *Biochemical Pharmacology*, *81*(2), 259–268. https://doi.org/10.1016/j.bcp.2010.09.025

Bayati, S., Yazdanparast, R., Majd, S. S., & Oh, S. (2011). Protective effects of 1,3-diaryl-2-propen-1-one derivatives against H_2O_2-induced damage in SK-N-MC cells. *Journal of Applied Toxicology*, *31*(6), 545–553. https://doi.org/10.1002/jat.1594

Bhat, A. H., Dar, K. B., Anees, S., Zargar, M. A., Masood, A., Sofi, M. A., & Ganie, S. A. (2015). Oxidative stress, mitochondrial dysfunction and neurodegenerative diseases; a mechanistic insight. *Biomedicine & Pharmacotherapy*, *74*, 101–110. https://doi.org/10.1016/j.biopha.2015.07.025

Boukamp, P., Petrussevska, R. T., Breitkreutz, D., Hornung, J., Markham, A., & Fusenig, N. E. (1988). Normal keratinization in a spontaneously immortalized aneuploid human keratinocyte cell line. *The Journal of Cell Biology*, *106*(3), 761–771. https://doi.org/10.1083/jcb.106.3.761

Brand, R. M., Wipf, P., Durham, A., Epperly, M. W., Greenberger, J. S., & Falo, L. D. Jr. (2018). Targeting mitochondrial oxidative stress to mitigate UV-induced skin damage. *Frontiers in Pharmacology*, *9*, 920. https://doi.org/10.3389/fphar.2018.00920

Caliş, B., Yerlikaya, F. H., Ataseven, A., Temiz, S. A., & Onmaz, D. E. (2022). Oxidative stress-related miRNAs in patients with severe acne vulgaris. *Indian Journal of Dermatology*, *67*(6), 657–661. https://doi.org/10.4103/ijd.ijd_467_22

Calniquer, G., Khanin, M., Ovadia, H., Linnewiel-Hermoni, K., Stepensky, D., Trachtenberg, A., Sedlov, T., Braverman, O., Levy, J., & Sharoni, Y. (2021). Combined effects of carotenoids and polyphenols in balancing the response of skin cells to UV irradiation. *Molecules*, *26*(7), 1931. https://doi.org/10.3390/molecules26071931

Colombo, I., Sangiovanni, E., Maggio, R., Mattozzi, C., Zava, S., Corbett, Y., Fumagalli, M., Carlino, C., Corsetto, P. A., Scaccabarozzi, D., Calvieri, S., Gismondi, A., Taramelli, D., & Dell'Agli, M. (2017). HaCaT cells as a reliable in vitro differentiation model to dissect the inflammatory/repair response of human keratinocytes. *Mediators of Inflammation*, *2017*, 7435621. https://doi.org/10.1155/2017/7435621

Deitersen, J., Berning, L., Stuhldreier, F., Ceccacci, S., Schlütermann, D., Friedrich, A., Wu, W., Sun, Y., Böhler, P., Berleth, N., Mendiburo, M. J., Seggewiß, S., Anand, R., Reichert, A. S., Monti, M. C., Proksch, P., & Stork, B. (2021). High-throughput screening for natural compound-based autophagy modulators reveals novel chemotherapeutic mode of action for arzanol. *Cell Death & Disease*, *12*(6), 560. https://doi.org/10.1038/s41419-021-03830-5

Del Gaudio, F., Pollastro, F., Mozzicafreddo, M., Riccio, R., Minassi, A., & Monti, M. C. (2018). Chemoproteomic fishing identifies arzanol as a positive modulator of brain glycogen phosphorylase. *Chemical Communications*, *54*(91), 12863–12866. https://doi.org/10.1039/c8cc07692h

Farshori, N. N., Saquib, Q., Siddiqui, M. A., Al-Oqail, M. M., Al-Sheddi, E. S., Al-Massarani, S. M., & Al-Khedhairy, A. A. (2021). Protective effects of *Nigella sativa* extract against H_2O_2-induced cell death through the inhibition of DNA damage and cell cycle arrest in human umbilical vein endothelial cells (HUVECs). *Journal of Applied Toxicology*, *41*(5), 820–831. https://doi.org/10.1002/jat.4126

Furlan, V., & Bren, U. (2023). *Helichrysum italicum*: From extraction, distillation, and encapsulation techniques to beneficial health effects. *Food*, *12*(4), 802. https://doi.org/10.3390/foods12040802

Gülçin, İ. (2010). Antioxidant properties of resveratrol: A structure–activity insight. *Innovative Food Science & Emerging Technologies*, *11*, 210–218. https://doi.org/10.1016/j.ifset.2009.07.002

Jiang, B. W., Zhang, W. J., Wang, Y., Tan, L. P., Bao, Y. L., Song, Z. B., Yu, C. L., Wang, S. Y., Liu, L., & Li, Y. X. (2020). Convallatoxin induces HaCaT cell necroptosis and ameliorates skin lesions in psoriasis-like mouse models. *Biomedicine & Pharmacotherapy*, *121*, 109615. https://doi.org/10.1016/j.biopha.2019.109615

Juliano, C., Marchetti, M., Campagna, P., & Usai, M. (2019). Antimicrobial activity and chemical composition of essential oil from *Helichrysum microphyllum* Cambess. subsp. *tyrrhenicum* Bacch., Brullo & Giusso collected in South-West Sardinia. *Saudi Journal of Biological Sciences*, *26*(5), 897–905. https://doi.org/10.1016/j.sjbs.2018.04.009

Kasugai, S., Hasegawa, N., & Ogura, H. (1990). A simple in vito cytotoxicity test using the MTT (3-[4,5]-dimethylthiazol-2-yl-2,5-diphenyl tetrazolium bromide) colorimetric assay: Analysis of eugenol toxicity on dental pulp cells (RPC-C2A). *Japanese Journal of Pharmacology*, *52*(1), 95–100. https://doi.org/10.1254/jjp.52.95

Lenzen, S., Lushchak, V. I., & Scholz, F. (2022). The pro-radical hydrogen peroxide as a stable hydroxyl radical distributor: Lessons from pancreatic beta cells. *Archives of Toxicology*, *96*(7), 1915–1920. https://doi.org/10.1007/s00204-022-03282-6

Liao, C., Wu, L., Zhong, W., Zheng, Q., Tan, W., Feng, K., Feng, X., & Meng, F. (2022). Cellular antioxidant properties of *Ischnoderma resinosum* polysaccharide. *Molecules*, *27*(22), 7717. https://doi.org/10.3390/molecules27227717

Liu, H. M., Cheng, M. Y., Xun, M. H., Zhao, Z. W., Zhang, Y., Tang, W., & Wang, W. (2023). Possible mechanisms of oxidative stress-induced skin cellular senescence, inflammation, and cancer and the therapeutic potential of plant polyphenols. *International Journal of Molecular Sciences*, *24*(4), 3755. https://doi.org/10.3390/ijms24043755

Liu, H. M., Tang, W., Lei, S. N., Zhang, Y., Cheng, M. Y., Liu, Q. L., & Wang, W. (2023). Extraction optimization, characterization and biological activities of polysaccharide extracts from *Nymphaea hybrid*. *International Journal of Molecular Sciences*, *24*(10), 8974. https://doi.org/10.3390/ijms24108974

Lushchak, V. I., & Storey, K. B. (2021). Oxidative stress concept updated: Definitions, classifications, and regulatory pathways implicated. *EXCLI Journal*, *20*, 956–967. https://doi.org/10.17179/excli2021-3596

Mahaseth, T., & Kuzminov, A. (2017). Potentiation of hydrogen peroxide toxicity: From catalase inhibition to stable DNA-iron complexes. *Mutation Research, Reviews in Mutation Research*, *773*, 274–281. https://doi.org/10.1016/j.mrrev.2016.08.006

Mammino, L. (2017). Intramolecular hydrogen bonding and conformational preferences of arzanol—An antioxidant acylphloroglucinol. *Molecules*, *22*(8), 1294. https://doi.org/10.3390/molecules22081294

Michalak, M. (2022). Plant-derived antioxidants: Significance in skin health and the ageing process. *International Journal of Molecular Sciences*, *23*(2), 585. https://doi.org/10.3390/ijms23020585

Michalak, M., Zagórska-Dziok, M., Klimek-Szczykutowicz, M., & Szopa, A. (2023). Phenolic profile and comparison of the antioxidant, anti-ageing, anti-inflammatory, and protective activities of *Borago officinalis* extracts on skin cells. *Molecules*, *28*(2), 868. https://doi.org/10.3390/molecules28020868

Mirata, S., Asnaghi, V., Chiantore, M., Salis, A., Benvenuti, M., Damonte, G., & Scarfì, S. (2023). Photoprotective and anti-aging properties of the apical frond extracts from the mediterranean seaweed *Ericaria amentacea*. *Marine Drugs*, *21*(5), 306. https://doi.org/10.3390/md21050306

Nichols, J. A., & Katiyar, S. K. (2010). Skin photoprotection by natural polyphenols: Anti-inflammatory, antioxidant and DNA repair mechanisms. *Archives of Dermatological Research*, *302*(2), 71–83. https://doi.org/10.1007/s00403-009-1001-3

Ornano, L., Venditti, A., Sanna, C., Ballero, M., Maggi, F., Lupidi, G., … Bianco, A. (2015). Chemical composition and biological activity of the essential oil from *Helichrysum microphyllum* Cambess. ssp. *tyrrhenicum* Bacch., Brullo e Giusso growing in La Maddalena Archipelago, Sardinia. *Journal of Oleo Science*, *64*(1), 19–26. https://doi.org/10.5650/jos.ess14171

Park, C., Lee, H., Noh, J. S., Jin, C. Y., Kim, G. Y., Hyun, J. W., … Choi, Y. H. (2020). Hemistepsin A protects human keratinocytes against hydrogen peroxide-induced oxidative stress through activation of the Nrf2/HO-1 signaling pathway. *Archives of Biochemistry and Biophysics*, *691*, 108512. https://doi.org/10.1016/j.abb.2020.108512

Pavelescu, L. A. (2015). On reactive oxygen species measurement in living systems. *Journal of Medicine and Life*, *8*, 38–42.

Petretto, G. L., Vacca, G., Addis, R., Pintore, G., Nieddu, M., Piras, F., Sogos, V., Fancello, F., Zara, S., & Rosa, A. (2023). Waste *Citrus limon* leaves as source of essential oil rich in limonene and citral: Chemical characterization, antimicrobial and antioxidant properties, and effects on cancer cell viability. *Antioxidants*, *12*(6), 1238. https://doi.org/10.3390/antiox12061238

Ransy, C., Vaz, C., Lombès, A., & Bouillaud, F. (2020). Use of H_2O_2 to cause oxidative stress, the catalase issue. *International Journal of Molecular Sciences*, *21*(23), 9149. https://doi.org/10.3390/ijms21239149

Rosa, A., Deiana, M., Corona, G., Atzeri, A., Incani, A., & Dessì, M. A. (2005). Cholesterol as target of Fe-NTA-induced lipid peroxidation in rat tissues. *Toxicology Letters*, *157*(1), 1–8. https://doi.org/10.1016/j.toxlet.2004.12.013

Rosa, A., Deiana, M., Atzeri, A., Corona, G., Incani, A., Melis, M. P., Appendino, G., & Dessì, M. A. (2007). Evaluation of the antioxidant and cytotoxic activity of arzanol, a prenylated alpha-pyrone-phloroglucinol etherodimer from *Helichrysum italicum* subsp. *microphyllum*. *Chemico-Biological Interactions*, *165*(2), 117–126. https://doi.org/10.1016/j.cbi.2006.11.006

Rosa, A., Pollastro, F., Atzeri, A., Appendino, G., Melis, M. P., Deiana, M., Incani, A., Loru, D., & Dessì, M. A. (2011). Protective role of arzanol against lipid peroxidation in biological systems. *Chemistry and Physics of Lipids*, *164*(1), 24–32. https://doi.org/10.1016/j.chemphyslip.2010.09.009

Rosa, A., Atzeri, A., Nieddu, M., & Appendino, G. (2017). New insights into the antioxidant activity and cytotoxicity of arzanol and effect of methylation on its biological properties. *Chemistry and Physics of Lipids*, *205*, 55–64. https://doi.org/10.1016/j.chemphyslip.2017.05.001

Saha, I., Roy, S., Das, D., Das, S., & Karmakar, P. (2023). Topical effect of polyherbal flowers extract on xanthan gum hydrogel patch-induced wound healing activity in human cell lines and male BALB/c mice. *Biomedical Materials*, *18*(3), 035016. https://doi.org/10.1088/1748-605X/acce89

Schikowski, T., & Krutmann, J. (2019). Luftverschmutzung (Feinstaub, Stickstoffdioxid) und Hautalterung [air pollution (particulate matter and nitrogen dioxide) and skin aging]. *Hautarzt*, *70*(3), 158–162. https://doi.org/10.1007/s00105-018-4338-8

Shimamoto, J., Kurokawa, T., Tanizaki, H., & Moriwaki, S. (2019). The evaluation of oxidative stress in patients with psoriasis vulgaris and atopic dermatitis by measuring the urinary level of 8-hydroxy-2′-deoxyguanosine. *Journal of Cutaneous Immunology and Allergy*, *2*(6), 163–168. https://doi.org/10.1002/cia2.12088

Sogos, V., Caria, P., Porcedda, C., Mostallino, R., Piras, F., Miliano, C., De Luca, M. A., & Castelli, M. P. (2021). Human neuronal cell lines as an in vitro toxicological tool for the evaluation of novel psychoactive substances. *International Journal of Molecular Sciences*, *22*(13), 6785. https://doi.org/10.3390/ijms22136785

Suroowan, S., Llorent-Martínez, E. J., Zengin, G., Buskaran, K., Fakurazi, S., Abdalla, A. N., Khalid, A., Le Van, B., & Mahomoodally, M. F. (2023). Unveiling the antioxidant, clinical enzyme inhibitory properties and cytotoxic potential of *Tambourissa peltata* baker—An understudied endemic plant. *Molecules*, *28*(2), 599. https://doi.org/10.3390/molecules28020599

Taglialatela-Scafati, O., Pollastro, F., Chianese, G., Minassi, A., Gibbons, S., Arunotayanun, W., Mabebie, B., Ballero, M., & Appendino, G. (2013). Antimicrobial phenolics and unusual glycerides from *Helichrysum italicum* subsp. *microphyllum*. *Journal of Natural Products*, *76*(3), 346–353. https://doi.org/10.1021/np3007149

Wang, C. C., Hsiao, C. Y., Hsu, Y. J., Ko, H. H., Chang, D. C., & Hung, C. F. (2022). Anti-inflammatory effects of cycloheterophyllin on dinitrochlorobenzene-induced atopic dermatitis in HaCaT cells and BALB/c mice. *Molecules*, *27*(9), 2610. https://doi.org/10.3390/molecules27092610

Winterbourn, C. C. (2013). The biological chemistry of hydrogen peroxide. *Methods in Enzymology*, *528*, 3–25. https://doi.org/10.1016/B978-0-12-405881-1.00001-X

Winterbourn, C. C. (2018). Biological production, detection, and fate of hydrogen peroxide. *Antioxidants & Redox Signaling*, *29*(6), 541–551. https://doi.org/10.1089/ars.2017.7425

Yan, Y., Chen, X., Huang, J., Huan, C., & Li, C. (2022). H_2O_2-induced oxidative stress impairs meat quality by inducing apoptosis and autophagy via ROS/NF-κB signaling pathway in broiler thigh muscle. *Poultry Science*, *101*(4), 101759. https://doi.org/10.1016/j.psj.2022.101759

Zhang, J., Wang, W., & Mao, X. (2020). Chitopentaose protects HaCaT cells against H_2O_2-induced oxidative damage through modulating MAPKs and Nrf2/ARE signaling pathways. *Journal of Functional Foods*, *72*, 104086. https://doi.org/10.1016/j.jff.2020.104086

How to cite this article: Piras, F., Sogos, V., Pollastro, F., Appendino, G., & Rosa, A. (2023). Arzanol, a natural phloroglucinol α-pyrone, protects HaCaT keratinocytes against H_2O_2-induced oxidative stress, counteracting cytotoxicity, reactive oxygen species generation, apoptosis, and mitochondrial depolarization. *Journal of Applied Toxicology*, 1–13. https://doi.org/10.1002/jat.4570